The Journal of Chemical Physics

RESEARCH ARTICLE | OCTOBER 27 2023

Phenylpropiolic acid isolated in cryogenic nitrogen and xenon matrices: NIR and UV-induced study FREE

S. Lopes ; T. Nikitin ; R. Fausto

J. Chem. Phys. 159, 164311 (2023)
https://doi.org/10.1063/5.0167128

AIP Publishing

The Journal of Chemical Physics ARTICLE pubs.aip.org/aip/jcp

Phenylpropiolic acid isolated in cryogenic nitrogen and xenon matrices: NIR and UV-induced study

Cite as: J. Chem. Phys. 159, 164311 (2023); doi: 10.1063/5.0167128
Submitted: 10 July 2023 • Accepted: 5 October 2023 •
Published Online: 27 October 2023

S. Lopes,[1,a] T. Nikitin,[1] and R. Fausto[1,2]

AFFILIATIONS

[1]CQC-IMS, Department of Chemistry, University of Coimbra, 3004-535 Coimbra, Portugal
[2]Faculty of Sciences and Letters, Department of Physics, Istanbul Kultur University, Ataköy Campus, Bakirköy, 34156 Istanbul, Türkiye

[a]Author to whom correspondence should be addressed: susylopes@qui.uc.pt

ABSTRACT

Phenylpropiolic acid ($C_6H_5C{\equiv}CCOOH$, PPA) isolated in nitrogen and xenon cryogenic matrices was studied by infrared spectroscopy. The experimental studies were complemented by a series of quantum chemical calculations carried out at the density functional theory (B3LYP) and MP2 levels of theory (with different basis sets). The calculations predicted the existence of two planar PPA conformers, differing in the arrangement of the carboxylic group. The higher-energy *trans*-PPA conformer has a negligible population in the gas phase at room temperature and was prepared *in situ* in the N_2 cryomatrix through vibrationally-induced rotamerization of the lower-energy *cis*-PPA conformer, achieved using selective narrowband infrared excitation of the OH stretching coordinate of the latter species. Broadband UV ($\lambda > 235$ nm) irradiation of matrix-isolated *cis*-PPA was also undertaken, leading to the observation of *cis*-PPA → *trans*-PPA isomerization. No other UV-induced photoreactions were observed. The *in situ* generated *trans*-PPA conformer was found to decay back to *cis*-PPA in the dark by tunneling, and its lifetimes under different experimental conditions were determined. The assignment of the infrared spectra of both conformers is presented, considerably extending the vibrational information available on this molecule.

I. INTRODUCTION

Phenylpropiolic acid ($C_6H_5C{\equiv}CCOOH$, PPA) is the phenyl derivative of propiolic acid ($HC{\equiv}CCOOH$, PA), in which the phenyl group replaces the acetylenic hydrogen atom. Like PA and other simple carboxylic acids,[1–3] PPA has two planar conformers (Fig. 1), where the carboxylic acid group adopts a *cis* orientation (O=C–O–H dihedral angle equal to 0°) or a *trans* orientation (O=C–O–H dihedral angle equal to 180°).

The biological importance of PPA and its derivatives is well known, as well as their relevance in chemical synthesis.[4–17] The bioactivity of this type of compound as potential therapeutic agents for type 2 diabetes was recently verified through the analysis of a series of novel GPR40 agonists bearing phenylpropiolic acid motifs,[4] and some PPA derivatives have also been suggested as potential drugs for cancer therapy.[5,6] PPA itself has been shown to act as an inhibitor of type II 17β-hydroxysteroid dehydrogenase (an enzyme that oxidizes many steroid substrates[7]) by increasing the local bone concentration of estradiol, which enhances bone quality and strength and is useful in treating osteoporosis.[18] The use of PPA in the synthesis of organic and organometallic compounds has widespread applications.[8–17] Examples include the palladium-catalyzed carbonylative synthesis of alkynones from aryl iodides and phenylpropiolic acid employing formic acid as the CO source,[9] one-pot synthesis of 4-phenylcoumarins by reaction with phenols in polyphosphoric acid in the presence of $Tl(OAc)_3$,[16] synthesis of vinyl sulfones through decarboxylation coupling reactions of sodium sulfinates with PPA,[14] and reactions of PPA derivatives in benzene and cyclohexane to give the corresponding 3,3-diphenylpropanoic acid derivatives under super electrophilic activation.[17] Other previous investigations on PPA include the study of the ^{13}C kinetic isotope effect in the decarboxylation of the compound in hydrogen-donating media[19] and the study of its thermodynamics of sublimation.[20]

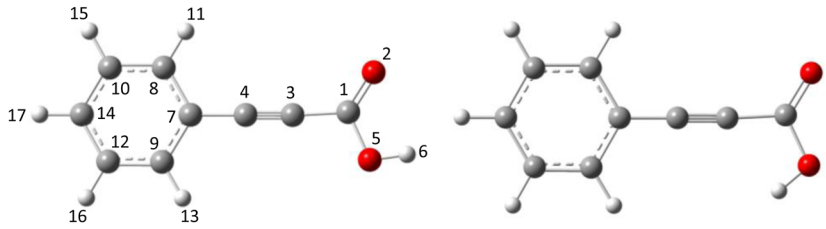

FIG. 1. *Cis*-PPA (*left*) and *trans*-PPA (*right*), including numbering of atoms adopted in this work. Color code: C, gray; H, white; O, red.

Rollett determined the crystal structure of PPA by x-ray diffractometry at room temperature in 1955,[21] while Das and Desiraju[22] investigated the effects of substitution at the aromatic ring on the conformational preferences and molecular packing of a series of PPA derivatives. Previously, another publication from the same group reported the stereoelectronic effects of substituent groups in several phenylpropiolic acids in the solid state.[23]

Zhou *et al.*[24] analyzed the gas-phase microwave spectrum of PPA and determined the rotational and the centrifugal distortion constants for *cis*-PPA, which were found to be in good agreement with those obtained using both density functional theory (DFT) and MP2 quantum chemical methods, with the aug-cc-pVTZ basis set.

In the present study, PPA was isolated in low-temperature nitrogen and xenon matrices and studied by infrared spectroscopy combined with quantum chemical calculations performed at different levels of theory. Xenon and nitrogen were chosen as matrix media to take advantage of the well-known ability of these materials to stabilize high-energy conformers of carboxylic acids.[1,2] The photochemical behavior of matrix-isolated monomeric PPA subjected to *in situ* broadband UV irradiation ($\lambda > 235$ nm) was investigated, revealing the occurrence of *cis*-PPA → *trans*-PPA photorotamerization as the sole observed process under the experimental conditions used. The higher-energy *trans* conformer could also be generated *in situ* by selective vibrational excitation of the lower-energy *cis* conformer using a tunable narrowband IR light source. The tunneling decay rates of *trans*-PPA under different experimental conditions were evaluated. Overall, this study enabled us to structurally and vibrationally characterize both PPA conformers, elucidate the UV- and IR-induced PPA conformational isomerization mechanisms, and evaluate the stability of the higher-energy *trans* conformer under various experimental conditions.

II. COMPUTATIONAL DETAILS AND RESULTS

A. Computational details

The quantum chemical calculations were performed using the Gaussian 09 (Rev. D.01)[25] and Gaussian 16 (Rev. B.01)[26] software packages at the DFT(B3LYP)[27–29] and MP2[30] levels of theory with the 6-311++G(d,p), 6-311++G(2df,2pd), 6-311++G(3df,3pd), and aug-cc-pVDZ basis sets.[31–36] A relaxed one-dimensional (1-D) potential energy scan was undertaken in order to locate the minima and the transition state structures for conformational isomerization. The nature of all described stationary points on the studied potential energy surface (PES) was characterized through the analysis of the corresponding Hessian matrices. The geometries were optimized using the TIGHT convergence criteria, and the vibrational frequencies and infrared intensities were calculated at the DFT(B3LYP) and MP2 levels of theory. To locate transition state structures for conformational interconversion, we utilized the synchronous transit-guided quasi-Newton (STQN) method.[37]

The calculated vibrational frequencies and IR intensities were used to assist in analyzing the experimental spectra. Throughout the manuscript, the calculated spectra obtained at the DFT(B3LYP)/6-311++G(3df,3pd) level of theory will be used as the reference theoretical data. The wavenumbers obtained by this method were scaled down by our standard scale factors for this combination of the method, functional, and basis set. Specifically, we used scale factors of 0.979 for wavenumbers below 3000 cm^{-1} and 0.940 for those above to correct for the effects of the basis set limitations, neglected part of electron correlation, and anharmonicity effects. The resulting (scaled) wavenumbers together with the calculated intensities were used to simulate the spectra shown in the figures. In these simulations, the absorptions were convoluted using a Lorentzian function with a full width at half maximum (FWHM) of 2 cm^{-1}. The vibrational analysis of all calculated species was supported by the animation of the vibration module provided by Chemcraft software (version 1.8).[38]

B. Computational results

1. Geometries and conformational energies

In the PPA molecule, there is only one conformationally relevant degree of freedom, which can be described as internal rotation of the hydroxyl group around the C–O bond. In consonance with previous reports,[21–24] the calculations carried out in the present study at different levels of theory indicate the existence of two low energy conformers of the compound, both belonging to the C_s symmetry point group (see Fig. 1), which correspond to the *cis* and *trans* arrangements of the O=C–O–H moiety. The present calculations confirm that the most stable conformer bears the O=C–O–H group in the *cis* orientation (O=C–O–H dihedral angle equal to 0°; *cis*-PPA), whereas in the higher-energy conformer, the O=C–O–H group is in the *trans* orientation (O=C–O–H dihedral angle equal to 180°; *trans*-PPA). As it is usually found for simple carboxylic acids,[39–42] the main factor responsible for stabilizing the *cis* conformer with respect to the *trans* conformer is the different relative orientation of the bond-dipoles associated with the highly-polarized O–H and C=O bonds in the two conformers: in the *cis* conformer, these bond-dipoles are nearly anti-parallel, while in the *trans* conformer they are aligned in an approximate parallel way. The relative

TABLE I. Electronic relative energies (including zero-point corrections) calculated at the DFT(B3LYP) and MP2 levels of theory for the two conformers of PPA (kJ mol^{-1}).

Method and basis set	Conformer	
DFT(B3LYP)/	*cis*-PPA	*trans*-PPA
6-311++G(d,p)	0.0	13.6
6-311++G(2df,2pd)	0.0	12.0
6-311++G(3df,3pd)	0.0	11.9
aug-cc-pVDZ	0.0	11.8
MP2/		
6-311++G(d,p)	0.0	14.9
6-311++G(2df,2pd)	0.0	11.9
6-311++G(3df,3pd)	0.0	12.1
aug-cc-pVDZ	0.0	11.2

calculated energies, with zero-point corrections, of the two PPA conformers calculated by DFT(B3LYP) and MP2 methods are presented in Table I. The optimized geometries of the two conformers of PPA are listed in Tables S1 and S2 (supplementary material).

As observed for other carboxylic acids,[39–42] the calculated C=O bond is longer in the most stable *cis* conformer than in the *trans* form [1.206 vs 1.198 Å; DFT(B3LYP)/6-311++G(3df,3pd) values], whereas the C–O bond follows the opposite trend, being shorter in *cis*-PPA than in *trans*-PPA (1.353 vs 1.358 Å). These findings verify enhanced π-electron delocalization within the carboxylic group of the *cis* conformer. This delocalization contributes to the stabilization of the *cis* conformer compared to the *trans* form. This can be understood by considering the above mentioned distinct bond-dipole/bond-dipole interactions in each conformer, which induce π-charge migration within this molecular fragment. In turn, the exocyclic C–C bond lengths are 1.435 and 1.443 Å (C1–C3) and 1.420 and 1.421 Å (C4–C7) in *cis*- and *trans*-PPA, respectively. The shorter C4–C7 bond lengths, compared to the C1–C3 bond lengths, express the larger double character of the first bond in both conformers. This difference highlights a greater π delocalization between the electron-donating phenyl group and the electron-accepting acetylenic moiety. In contrast, the π delocalization is lesser between the acetylenic fragment (acting as the donor) and the carbonyl group (serving as the acceptor). Such result could be anticipated, considering that π electron donation from the acetylenic group to the carbonyl moiety suffers competition from the above-mentioned π electron donation from the acid oxygen atom. The relative values of the C1–C3 bond length in *cis*- and *trans*-PPA can also be explained following this line of reasoning: since the π electron donation from the acid oxygen to the carbonyl bond is more extensive in the *cis* conformer, the π electron donation from the acetylenic group becomes less important, justifying the longer C1–C3 bond length in *cis*-PPA. The different bond-dipole/bond-dipole interactions within the carboxylic group in the two conformers do also justify the longer O–H bond length in the *cis* conformer (0.968 Å, vs 0.965 Å in *trans*-PPA), since the nearly antiparallel alignment of the O–H and C=O bond dipoles tends to polarize more the O–H bond in the *cis* conformer than in the *trans* form, where, as mentioned above, these dipoles are nearly parallel.

Figure S1 shows the potential energy profile associated with the internal rotation around the C–O bond corresponding to the interconversion between the two conformers of PPA. The relative energy difference between the two forms predicted by the DFT(B3LYP) and MP2 methods is in the ranges 11.8–13.6 kJ mol^{-1} and 11.2–14.9 kJ mol^{-1}, respectively (see Table I). On the other hand, the *trans*-PPA → *cis*-PPA energy barrier was predicted to be around ~30 kJ mol^{-1} (~42 kJ mol^{-1}, in the reverse direction).

Considering the calculated relative stabilities of the *cis* and *trans* conformers of PPA, the expected gas phase equilibrium populations at room temperature were estimated to be ~99.6% and ~0.4%, respectively, i.e., the calculations suggest the sole presence of the most stable *cis*-PPA conformer in the as-deposited cryogenic Xe and N_2 matrices. As described in detail in Sec. III, the experimental data confirm these theoretical predictions.

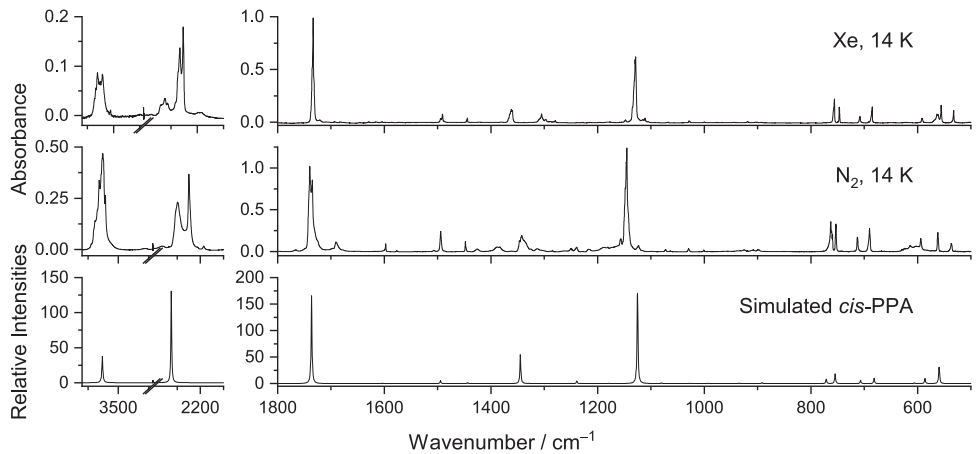

FIG. 2. The experimental IR spectra of PPA isolated in Xe and N_2 matrices after deposition at 14 K, compared with the theoretical IR spectrum of *cis*-PPA calculated at the DFT(B3LYP)/6-311++G(3df,3pd) level of theory. The calculated harmonic frequencies were scaled by 0.979 and 0.94 for regions below and above 3000 cm^{-1}, respectively.

III. EXPERIMENTAL DETAILS AND RESULTS

A. Experimental details

The matrices were prepared by co-depositing sublimated phenylpropiolic acid (purity >99%, sourced from Aldrich) with a significant excess of the matrix host gas (estimated ratio of ~1:750). The gases used were N_2 (N60) and Xe (N48), both obtained from Air Liquide. The deposition occurred onto a CsI substrate attached to the cold tip of the cryostat — an APD Cryogenics closed-cycle helium refrigeration system equipped with a DE-202A expander. For the N_2 matrix, the substrate temperature during matrix deposition was maintained at 14 K, whereas it was kept at 25 K for the Xe matrix. These deposition temperatures were chosen to optimize the optical properties of the matrix in each case. For deposition, the compound was housed in a specially designed, homemade temperature-variable mini-oven connected to the cryostat via a needle valve. The oven's internal temperature, utilized for the sublimation of the compound (~353–358 K), was monitored by a thermocouple. Meanwhile, the valve nozzle was maintained at room temperature (298 K). The temperature of the CsI substrate of the cryostat was measured directly at the sample holder using a silicon diode sensor connected to a digital temperature controller (LakeShore 335) with an accuracy of 0.1 K.

The IR spectra were recorded in the 4000–400 cm^{-1} mid-IR range with a spectral resolution of 0.5 cm^{-1} using a Thermo Nicolet 6700 Fourier transform infrared spectrometer. This spectrometer was outfitted with a deuterated triglycine sulfate (DTGS) detector, a potassium bromide (KBr) beam splitter, and an ETC EverGlo globar source. For measurements in the 7500–4000 cm^{-1} near-IR region with a resolution of 1.0 cm^{-1}, we used a cooled indium gallium arsenide (InGaAS) detector, a calcium fluoride (CaF_2) beam splitter, and a white light source. To prevent interference from atmospheric H_2O and CO_2, the optical path of the spectrometer was continuously purged with dry CO_2-filtered air.

The matrices underwent broadband irradiation using UV light ($\lambda > 235$ nm, determined by the onset of KBr transmission in UV) from a 200 W high-pressure Hg(Xe) lamp (Newport, Oriel Instruments). A water filter positioned in front of the lamp absorbed the IR emission of the lamp. In the NIR region, the matrices were irradiated by an idler beam of an optical parametric oscillator Spectra Physics Quanta-Ray MOPO-SL (fwhm 0.2 cm^{-1}, pulse energy ~10 mJ) pumped with a pulsed Nd:YAG laser (10 ns, repetition rate 10 Hz). The free OH overtone of monomeric *cis*-PPA was excited to generate *trans*-PPA.

The kinetic studies of conversion of *trans*-PPA to *cis*-PPA in N_2 matrix were carried out in the dark at 14 K. Two different experimental conditions were used for the data collection: without any filter and with a cutoff filter inserted between the cryostat and the Globar source. The filter blocked the IR radiation from the spectrometer Globar source with energy above 4000 cm^{-1}, which could accelerate the *trans*-to-*cis* conversion.

B. Experimental results

1. Infrared spectra of matrix-isolated PPA

The infrared spectra of PPA isolated in nitrogen and xenon matrices are presented in Fig. 2, respectively. As stated in Sec. II B, according to the calculated large energy difference between the two conformers of PPA, the presence of only the most stable *cis* conformer in the cryogenic matrices could be anticipated. These expectations were fully confirmed, with the spectra of PPA isolated in both studied cryogenic matrices (N_2 and Xe) being very well reproduced by the calculated spectrum of this conformer [Fig. 2]. The proposed assignments of the IR fundamental bands of *cis*-PPA are listed in Table II. In both matrices, several bands, in particular the most intense ones that are related with vibrations of the more polar moieties (O–H; C=O; C–O) within the molecule, show extensive matrix-splitting, which is a common feature observed in the IR spectra obtained under matrix isolation conditions.

The OH stretching mode gives rise to a multiplet of bands observed at 3539.0/3532.0/3526.0/3521.5 and 3534.0/3531.035 25.5/3521.0 cm^{-1} (calculated: 3526.5 cm^{-1}) in the spectra obtained in N_2 and Xe, respectively, while the C=O stretching vibration originates the multiplet of bands at 1740.0/1738.0/1736.5/1735.0 (N_2) and 1735.0/1733.5/1732.0 (Xe) cm^{-1} (calculated: 1736.5 cm^{-1}), and the C–O stretching vibration (theory: 1125.2 cm^{-1}) gives rise to the two triplets of bands of high intensity observed at 1148.0/1146.0/1145.0 (N_2) and 1135.0/1130.0/1129.0 (Xe) cm^{-1}. Matrix splitting is also observed in the case of the features ascribed to the in-plane COH bending vibration [δ(COH)], which gives rise to the multiplets observed at 1346.0/1342.0/1335.0 and 1305.0/1298.0 cm^{-1} for the N_2 and Xe matrices, respectively, whereas the C≡C stretching vibration is experimentally observed as doublets at 2249.0/2225.0 (N_2) and 2233.0/2227.0 (Xe) cm^{-1} (calculated: 2262.9 cm^{-1}).

2. In situ narrowband near-IR irradiation of cis-PPA (2νOH; 6880.5 cm^{-1})

Conformers *cis*- and *trans*-PPA can be interconverted by internal rotation around the C–O bond. A general strategy was developed in our laboratory and others for selectively inducing this type of transformations in carboxylic acids (and other molecules containing the OH fragment), where narrowband selective excitation of a precursor conformer with near-IR light tuned at the frequency of the first overtone of its OH stretching vibration is used to promote its conversion into another conformer differing in the orientation of the OH group.[1,2,43] Following this strategy, we subjected the matrix-isolated (N_2) *cis*-PPA conformer to *in situ* near-IR irradiation at 6880.5 cm^{-1}, which corresponds to the first overtone of the OH stretching mode of *cis*-PPA, whose fundamental is observed at 3539.0/3532.0/3526.0/3521.5 cm^{-1} (see Table II). Figure S2 (supplementary material) shows a fragment of the near-IR experimental spectrum of PPA isolated in an N_2 matrix, compared with the anharmonic simulated spectrum of conformer *cis*-PPA in the same spectral region, which allows to clearly assign the experimental band observed at 6880.5 cm^{-1} to the 2ν(OH) mode of *cis*-PPA.

Figure 3(a) presents the experimental difference IR spectrum obtained by subtracting the spectrum of the as-deposited PPA in N_2 matrix from the spectrum recorded after excitation (6880.5 cm^{-1}). This spectrum is compared with the simulated difference IR spectrum generated from the calculated spectra of the two PPA conformers (*trans*-PPA *minus cis*-PPA) [Fig. 3(b)]. Irradiation at 6880.5 cm^{-1} for 90 min reduced the intensity of the bands belonging to the *cis*-PPA conformer by ~53%, while distinct new bands emerged in the spectrum, which perfectly fit the predicted spectrum of *trans*-PPA, thus demonstrating the near-IR induced *cis*-PPA → *trans*-PPA isomerization.

TABLE II. Experimental (matrix-isolation; N_2 and Xe) and DFT(B3LYP)/6-311++G(3df,3pd) calculated infrared spectra of conformer *cis*-PPA and vibrational assignments.[a]

Experimental		Calculated		Approximate description[b]
$\nu(N_2)$[c]	ν(Xe)[c]	ν	I^{IR}	
3539.0/3532.0/3526.0/3521.5	3534.0/3531.0/3525.5/3521.0	3526.5	118.8	ν(OH)
3068.0/3064.0	3068.0	3012.6	4.5	ν_1(CH)
3078.0	3059.0	3009.5	8.8	ν_2(CH)
3047.0	3039.0	3001.3	10.5	ν_3(CH)
3032.0	3023.0	2992.4	4.2	ν_4(CH)
n.obs.	n.obs.	2982.9	0.1	ν_5(CH)
2249.0/2225.0	2233.0/2227.0	2262.9	412.9	ν(CDC)
1740.0/1738.0/1736.5/1735.0	1735.0/1733.5/1732.0	1736.5	520.6	ν(C=O)
n.obs.	n.obs.	1603.5	2.8	$\nu_1(CC)_r$
n.obs.	n.obs.	1573.2	0.7	$\nu_2(CC)_r$
1494.0/1487.0	1495.0/1494.0/1491.0/1488.0	1494.6	18.2	$\nu_3(CC)_r$
1448.0	1145.0/1444.0	1443.7	6.4	$\nu_4(CC)_r$
1346.0/1342.0/1335.0	1305.0/1298.0	1344.9	174.0	δ(COH); ν(C–O)
1325.0	1288.0	1329.3	1.6	δ_1(CH)
1289.0/1285.0	1283.0/1279.0	1286.3	1.0	$\nu_5(CC)_r$
1239.0	1239.0	1238.9	15.4	δ(COH); ν(C4C7); ν(C1C3)
1180.0	1177.0	1179.5	2.1	δ_2(CH)
1156.5	1158.5	1162.2	0.2	δ_3(CH)
1148.0/1146.0/1145.0	1135.0/1130.0/1129.0	1125.2	562.0	ν(C–O); δ(COH);
1072.0	n.obs.	1080.6	4.1	δ_4(CH)
1029.0/1028.0	1029.0/1027.0	1027.4	2.5	$\nu_6(CC)_r$
n.obs.	n.obs.	996.4	0.0	γ_1(CH)
1001.0	1000.0	992.0	2.1	$\delta_1(CC)_r$
n.obs.	n.obs.	981.3	0.0	γ_2(CH)
927.0/925.0/924.0	920.0/918.0	934.5	2.8	γ_3(CH)
890.0/897.5	895.0/893.0	891.6	6.4	ν(C1C3); $\delta_2(CC)_r$
n.obs.	n.obs.	844.7	0.0	γ_4(CH)
763.0/762.0/761.0/759.5	758.0/757.0/756.0	771.3	28.2	γ_5(CH)
754.0/753.0	747.0	754.6	57.9	γ(C=O)
713.0	709.0/708.0	707.0	19.7	δ(OCO)
691.0/689.0	686.0/685.0	681.5	31.7	τ_1(Ph)
629.0	n.obs.	627.8	0.3	$\delta_3(CC)_r$; δ(C1C≡C); δ(C≡CC7)
614.0	n.obs.	606.1	4.2	$\delta_3(CC)_r$; δ(C1C≡C); δ(C≡CC7)
595.0	592.0/591.0	586.1	30.8	τ(OH)
562.0	563.0/562.0/556.0	559.9	53.6	δ(CC=O)
532.0	537.0	559.2	58.9	τ_2(Ph); τ(OH)
507.0	504.0	503.4	1.0	δ(C≡CC7); wag(Ph)
n.obs.	n.obs.	401.1	0.0	τ_3(Ph)
n.i.	n.i.	392.6	0.0	γ(C≡CC7)
n.i.	n.i.	301.2	0.6	δ_4(CC)r
n.i.	n.i.	192.9	0.6	γ(COOH)
n.i.	n.i.	182.6	1.8	δ(C≡CC7); δ(C1C≡C)
n.i.	n.i.	69.3	0.8	γ(Ph)
n.i.	n.i.	60.0	1.1	wag(COOH)
n.i.	n.i.	32.6	1.4	τ(CC)

[a]Frequencies (ν) in cm^{-1}; calculated intensities (I^{IR}) in km mol^{-1}.
[b]ν, stretching; δ, bending; γ, rocking; τ, torsion; wag, wagging; ph, phenyl; r, ring mode. All in-plane modes are A′ symmetry; all out-of-plane modes are A″ symmetry.
[c]n.obs, not observed; n.i., not investigated.

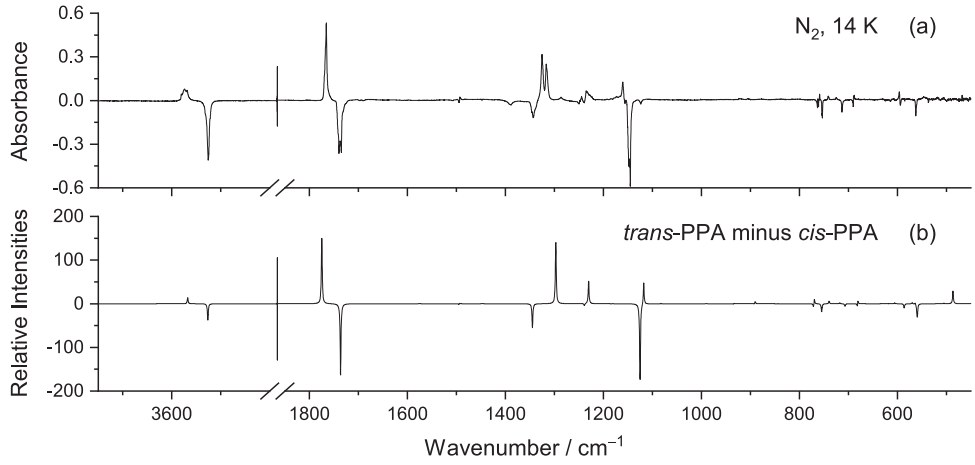

FIG. 3. Experimental difference IR spectrum of PPA: spectrum obtained after excitation at 6880.5 cm^{-1} (N_2; 90 min) *minus* the spectrum of the as-deposited PPA matrix (a), compared to the simulated difference infrared spectrum built using the DFT calculated spectra of the two conformers: *trans*-PPA *minus cis*-PPA (b).

The assignments of the fundamental bands of *trans*-PPA are presented in Table III. As usually for *trans* carboxylic acid conformers,[1,2] and in agreement with the structural data discussed above and also with the results of the vibrational calculations, both the ν(OH) and ν(C=O) modes are observed at higher frequencies for *trans*-PPA than for *cis*-PPA. The C≡C stretching is observed at 2242.0 cm^{-1} in *trans*-PPA, i.e., at a frequency lying at an intermediate value of those of the two component bands assigned to the same vibration in *cis*-PPA (2249.0 and 2225.0 cm^{-1}). The calculated frequencies for the two conformers, *trans* and *cis*-PPA, are 2250.4 and 2262.9 cm^{-1}, respectively. Other intense vibrations of *trans*-PPA are predicted by the calculations at 1297.2, 1230.2, and 1117.7 cm^{-1}, which correspond to the vibrations with major contributions of the ν(C–O), δ(COH), and δ(OCO) coordinates (see Table III). These modes correlate with the experimentally observed bands at 1334.0/1325.0/1317.0, multiplet in the range 1245–1220, and 1160.0 cm^{-1}, respectively. The OH torsional vibration in *trans*-PPA is observed at 506.0 cm^{-1}, in good agreement with the calculated value of 486.5 cm^{-1}, and at considerably lower frequency than the same mode in *cis*-PPA (observed: 595.0 cm^{-1}; calculated 586.1 cm^{-1}) as found before for other carboxylic acids, like formic, acetic, and propiolic acids.[1,2]

3. Broadband UV irradiation experiments (λ > 235 nm)

The broadband UV irradiation ($\lambda > 235$ nm) of the as-deposited PPA matrices also led to conversion of *cis*-PPA into *trans*-PPA (see Fig. S3; supplementary material). The spectral changes were already clearly visible after 1 min of irradiation, whereas about 38% of the original compound was consumed after 40 min of irradiation. The results of the UV irradiation of PPA in a xenon matrix mirror those observed in the nitrogen matrix. In both cases, no other photolysis products were observed, namely, the typical photoreactions observed for carboxylic acids, such as those resulting from either decarbonylation or decarboxylation of the compound.

Figure 4 depicts the experimental IR spectrum of PPA isolated in an N_2 matrix in the characteristic OH stretching region after deposition at 14 K and the changes that occurred as a result of UV irradiation of the matrix for 40 min. The figure also shows the observed changes resulting from the near-IR irradiation performed at 6880.5 cm^{-1}, as discussed in Sec. III B 2. It is worth noting that the profiles of the OH stretching absorption of both the reactant and product conformer change differently in the two types of experiments; and in particular, in the case of the *cis*-PPA conformer, the initial profile of the band is not kept in any of the experiments. Because the multiplet structure of the bands can be ascribed to the existence of multiple different matrix sites, the narrowband near-IR excitation could easily be anticipated to lead to changes in the *cis*-PPA band profile, since excitation of the molecules in different sites was not performed with equal efficiency (molecules in different sites absorb differently at the excitation wavelength). On the other hand, the observation of a similar effect as a result of the broadband UV irradiation is noteworthy, since it indicates that the matrix-site dependency of the efficiency of the transformation does also operate in this case, in spite of the expected large superposition of the absorbance bands of the different species in the UV and of the much higher-energy of the excitation light compared to near-IR. These results are in line with those previously reported for the parent compound, unsubstituted propiolic acid (PA), where irradiation of the matrix-isolated (N_2) compound with broadband UV light led to *cis* → *trans* isomerization and conversion between different matrix sites of the *cis*-PA conformer.[2]

4. Trans-PPA → cis-PPA tunneling decay

The amount of photogenerated *trans*-PPA slowly decreased after turning off the irradiation sources and keeping the sample in the dark. The decrease of the intensity of the bands due to this conformer was accompanied by an increase of intensity of the bands of *cis*-PPA, indicating that the higher-energy *trans*-PPA conformer was being transformed into the more stable *cis*-PPA form. Considering the experimental conditions, in particular the low

TABLE III. Experimental (matrix-isolation; N_2) and DFT(B3LYP)/6-311++G(3df,3pd) calculated infrared spectra of conformer *trans*-PPA and vibrational assignments.[a]

Experimental	Calculated		Approximate description[b]
$\nu(N_2)$[c]	ν	I^{IR}	
3580.5/3574.0/3569.0	3567.6	43.9	ν(OH)
n.obs.	3012.9	4.3	ν_1(CH)
n.obs.	3008.9	9.7	ν_2(CH)
n.obs.	3001.5	9.7	ν_3(CH)
n.obs.	2992.9	3.0	ν_4(CH)
n.obs.	2983.8	0.2	ν_5(CH)
2242.0	2250.4	337.9	ν(C≡C)
1766.0	1774.8	483.1	ν(C=O)
n.obs.	1603.5	2.0	$\nu_1(CC)_r$
n.obs.	1573.4	0.9	$\nu_2(CC)_r$
n.obs.	1494.2	15.7	$\nu_3(CC)_r$
n.obs.	1443.8	6.3	$\nu_4(CC)_r$
n.obs.	1329.4	0.8	$\nu_5(CC)_r$
1334.0/1325.0/1317.0	1297.2	450.9	δ(COH); ν(C–O)
n.obs.	1286.2	1.1	$\nu_6(CC)_r$
1244.5/1235.0/1233.0/1230.5/1227.0/1223.0	1230.2	166.4	δ(COH); ν(C4C7)
1173.0	1179.6	2.3	δ_1(CH)
n.obs.	1162.7	0.2	δ_2(CH)
1160.0	1117.7	162.9	ν(C–O); δ(OCO)
n.obs.	1081.1	4.5	δ_3(CH)
1028.0	1027.4	2.3	δ_4(CH)
n.obs.	996.8	0.0	γ_1(CH)
1001.0	991.8	2.2	$\delta_1(CC)_r$
n.obs.	980.7	0.0	γ_2(CH)
923.0	933.0	2.7	γ_3(CH)
906.0	890.3	17.8	ν(C1C3); $\delta_2(CC)_r$
n.obs.	843.6	0.0	γ_4(CH)
759.0	769.4	36.8	γ_5(CH)
741.0/740.0	739.3	18.7	γ(C=O)
725.0	717.7	7.3	δ(OCO); $\delta_3(CC)_r$
689.0/688.0	680.5	32.5	τ_1(Ph)
n.obs.	627.3	1.6	$\delta_3(CC)_r$; δ(C1C≡C); δ(C≡CC7)
596.0	605.8	10.1	$\delta_3(CC)_r$; δ(C1C≡C); δ(C≡CC7)
546.0	569.8	9.0	δ(CC = O)
546.0	563.7	10.1	γ(C≡CC7)
516.0	504.8	4.5	δ(C≡CC7); wag(Ph)
506.0	486.5	92.2	τ(OH)
n.i.	400.3	0.1	τ2(Ph)
n.i.	388.7	4.3	τ_3(Ph)
n.i.	299.5	0.3	δ_4(CC)r
n.i.	189.7	2.4	γ(Ph)
n.i.	177.5	4.9	δ(C≡CC7); δ(C1C≡C)
n.i.	68.9	0.5	γ(COOH)
n.i.	60.6	2.8	wag(COOH)
n.i.	26.7	4.6	τ(CC)

[a]Fequencies (ν) in cm^{-1}; calculated intensities (I^{IR}) in km mol^{-1}.
[b]ν, stretching; δ, bending; γ, rocking; τ, torsion; wag, wagging; ph, phenyl; r, ring mode. All in-plane modes are A′ symmetry; all out-of-plane modes are A″ symmetry.
[c]n.obs, not observed; n.i., not investigated.

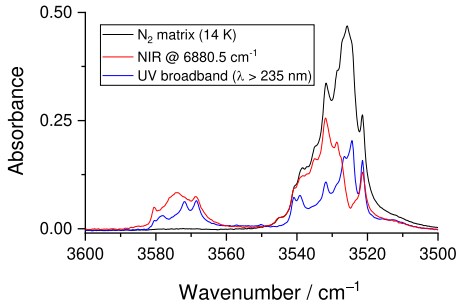

FIG. 4. Experimental FTIR spectra of PPA isolated in N_2 matrix after deposition (black), after excitation at 6880.5 cm^{-1} (N_2) (red), and after broadband UV irradiation (λ > 235 nm) in the OH stretching region (blue).

temperature (14 K) and absence of any additional energy source, it can easily be concluded that the observed spontaneous rotamerization occurred via the tunneling mechanism. Such decay of higher-energy *trans* carboxylic acid conformers into the more stable *cis* carboxylic forms has been observed many times for other carboxylic acids.[1–3,43]

The study of the tunneling decay of *trans*-PPA in an N_2 matrix was performed using different experimental conditions: with spectra being recorded (i) without any filter and (ii) with a cutoff filter blocking the IR radiation from the spectrometer Globar source with energy above 4000 cm^{-1}. The lifetime of the *trans*-PPA conformer was found to be ~4 h 17 min and 3 h 30 min, when measured with and without using the cutoff filter, respectively, and following excitation of *cis*-PPA at 6880.5 cm^{-1} (Fig. 5; see supplementary material for further experimental details). These results mean that the higher-frequency IR light provided by the Globar source of the spectrometer also promotes the *trans*-PPA → *cis*-PPA reaction (through near-IR induced conversion similarly to the *cis*-PPA → *trans*-PPA described above), or by facilitating the tunneling by promoting the *trans*-PPA conformer to a vibrationally excited torsional state, thus reducing the effective size of the torsional barrier through which the tunneling takes place.

It is worth mentioning that in the case of the parent molecule, propiolic acid, the decay time was also found to vary according to the different experimental conditions applied (particularly when the spectra were collected with or without a cutoff filter blocking the higher-energy IR radiation of the Globar source). However, the lifetimes of the *trans*-PA conformer were found to be considerably smaller than those now determined for *trans*-PPA: 38 min (21 min in the absence of a cutoff filter) after irradiation at 6874.9 cm^{-1} (site 2), and ~1 h 37 min when irradiation was performed at 6898.6 cm^{-1} (site 1; no cutoff filter).[2]

These results are in consonance with previously measured lifetimes in cryogenic matrices for other *trans* carboxylic acid conformers, which have shown that the stabilities of these species may be highly dependent on the trapping site.[44–46]

IV. CONCLUSION

In the present work, phenylpropiolic acid (PPA) was isolated in low temperature N_2 and xenon matrices and studied by quantum chemical calculations carried out at the DFT and MP2 levels of theory. In agreement with the computationally predicted conformational energy differences, only the most stable *cis*-PPA conformer was found to be present in the as-deposited matrices. Its IR spectra in both media were easily assigned with the help of the vibrational data obtained computationally.

Through the excitation of the first overtone of the OH stretching mode of the *cis*-PPA conformer, using narrowband near-IR light *in situ* irradiation, the higher-energy conformer, *trans*-PPA, was successfully produced. The same transformation (of *cis*-PPA into *trans*-PPA) could also be achieved upon irradiation of the as-deposited matrices (both N_2 and Xe) using broadband UV irradiation (λ > 235 nm). The two types of radiation-induced rotamerization processes (by near-IR vibrational excitation or UV electronic excitation of *cis*-PPA) were found to be dependent on the matrix-site environment, with *cis*-PPA molecules trapped in different matrix sites reacting with different efficiencies/rates.

The *trans*-PPA form, once generated *in situ*, spontaneously decays to the more stable *cis*-PPA form through the hydrogen atom tunneling mechanism. The decay time of *trans*-PPA produced

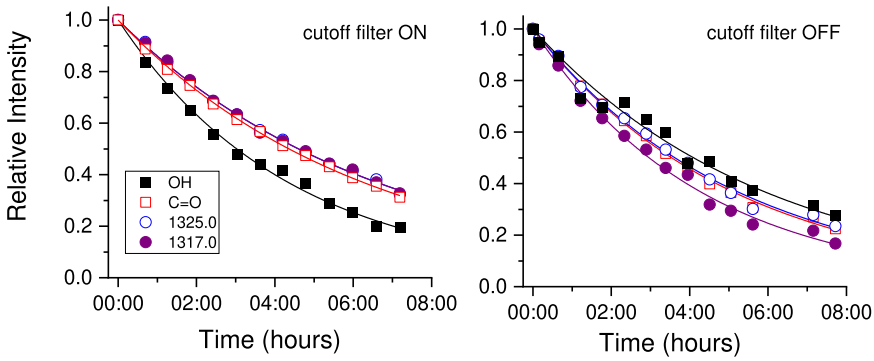

FIG. 5. Tunneling decay of *trans*-PPA in an N_2 matrix at 14 K. The decay of *trans*-PPA was evaluated using the bands at 3580.5/3574.0/3569.0 cm^{-1} (OH stretching, full squares), 1766.0 cm^{-1} (C=O stretching, open squares), 1325.0 and 1317.0 cm^{-1} (δ(COH)/ν(C–O), open circles and full circles, respectively) after irradiation at 6880.5 cm^{-1} (with and without using a >4000 cm^{-1} cutoff filter). The results were fitted with single exponential functions. See supplementary material for additional experimental details.

in N_2 matrix media upon excitation of the *cis*-PPA conformer at 6880.5 cm^{-1} was found to vary according to the experimental conditions used to record the spectra; in particular, the presence or absence of a cutoff filter blocking the higher-energy radiation of the Globar source of the spectrometer (>4000 cm^{-1}). These results indicate that the higher-frequency IR light provided by the Globar source of the spectrometer also promotes the *trans*-PPA → *cis*-PPA reaction through near-IR induced conversion similarly the *cis*-PPA → *trans*-PPA described above, or by facilitating the tunneling by promoting the *trans*-PPA conformer to a vibrationally excited torsional state, thus reducing the effective size of the torsional barrier through which the tunneling takes place.

Compared to the unsubstituted propiolic acid, the lifetimes of *trans*-PPA (~4 h 17 min and 3 h 30 min after excitation at 6880.5 cm^{-1}, with and without filter, respectively), were found to be significantly longer [*trans*-PA:[2] 38 and 21 min, with and without a cutoff filter, respectively, after irradiation at 6874.9 cm^{-1} (site 2), and around 1 h 37 min following irradiation at 6898.6 cm^{-1} (site 1; no filter)]. These results do not correlate with the energy barriers for the *trans* → *cis* rotamerization in the two molecules as free species in vacuum, which have been calculated to be about 30 kJ mol^{-1} in both cases, thus highlighting the relevance of local environment (matrix site) effects in determining the tunneling probability of the higher-energy conformers to decay into their corresponding lower-energy partners.

SUPPLEMENTARY MATERIAL

Figure S1, showing the calculated DFT(B3LYP) potential energy profile for internal rotation of the carboxylic group around the C–O bond corresponding to the interconversion between the two conformers of phenylpropiolic acid; Fig. S2, showing a fragment of the near-IR experimental spectrum of phenylpropiolic acid in N_2 matrix, compared with the simulated anharmonic spectra for the *cis*-PPA conformer; Fig. S3, with the calculated IR spectrum of *trans*- and *cis*- PPA, and the experimental difference IR spectrum obtained by subtracting the spectrum of the as-deposited PPA matrix (N_2; 14 K) from the spectrum registered after broadband UV irradiation (λ > 235 nm; 40 min); Tables S1 and S2, with the DFT and MP2 calculated optimized bond lengths and angles for the *cis*- and *trans*-PPA conformers; Tunneling decay details.

ACKNOWLEDGMENTS

This work has run within the research Project No. PTDC/QUI-QFI/1880/2020. The CQC-IMS is supported by the Fundação para a Ciência e a Tecnologia (FCT), through Project Nos. UI0313B/QUI/2020, UI0313P/QUI/2020, and LA/P/0056/2020. The authors also acknowledge the Laboratory for Advanced Computing at University of Coimbra (https://www.uc.pt/lca) for providing computing resources.

AUTHOR DECLARATIONS

Conflict of Interest

The authors have no conflicts to disclose.

Author Contributions

S. Lopes: Formal analysis (equal); Investigation (equal); Writing – original draft (equal); Writing – review & editing (equal). **T. Nikitin**: Formal analysis (equal); Investigation (equal); Writing – original draft (equal); Writing – review & editing (equal). **R. Fausto**: Funding acquisition (lead); Resources (equal); Supervision (equal); Writing – review & editing (equal).

DATA AVAILABILITY

The data that support the findings of this study are available from the corresponding author upon reasonable request.

REFERENCES

[1]S. Lopes, A. V. Domanskaya, R. Fausto, M. Räsänen, and L. Khriachtchev, "Formic and acetic acids in a nitrogen matrix: Enhanced stability of the higher-energy conformer," J. Chem. Phys. **133**, 144507 (2010).
[2]S. Lopes, T. Nikitin, and R. Fausto, "Propiolic acid in solid nitrogen: NIR- and UV-induced *cis* → *trans* isomerization and matrix-site-dependent *trans* → *cis* tunneling," J. Phys. Chem. A **123**, 1581–1593 (2019).
[3]S. Amiri, H. P. Reisenauer, and P. R. Schreiner, "Electronic effects on atom tunneling: Conformational isomerization of monomeric *para*-substituted benzoic acid derivatives," J. Am. Chem. Soc. **132**, 15902–15904 (2010).
[4]X. W. Jiang, B. E. Jiang, H. Liu, Z. T. Liu, L. L. Hu, M. Liu, W. Lu, and H. K. Zhang, "Design, synthesis, and biological evaluations of phenylpropiolic acid derivatives as novel GPR40 agonists," Eur. J. Med. Chem. **158**, 123–133 (2018).
[5]V. Indira Chandran, L. Matesic, J. M. Locke, D. Skropeta, M. Ranson, and K. L. Vine, "Anti-cancer activity of an acid-labile *N*-alkylisatin conjugate targeting the transferrin receptor," Cancer Lett. **316**, 151–156 (2012).
[6]X. Gao, J. Tang, H. Liu, L. Liu, L. Kang, and W. Chen, "Structure–activity relationship investigation of tertiary amine derivatives of cinnamic acid as acetylcholinesterase and butyrylcholinesterase inhibitors: Compared with that of phenylpropionic acid, sorbic acid and hexanoic acid," J. Enzyme Inhib. Med. Chem. **33**, 519–524 (2018).
[7]J. Wood, C. M. Bagi, C. Akuche, A. Bacchiocchi, J. Baryza, M. L. Blue, C. Brennan, A. M. Campbell, S. Choi, J. H. Cook, P. Conrad, B. R. Dixon, P. P. Ehrlich, T. Gane, D. Gunn, T. Joe, J. S. Johnson, J. Jordan, R. Kramss, P. Liu, J. Levy, D. B. Lowe, I. McAlexander, R. Natero, A. M. Redman, W. J. Scott, C. Town, and D. Poirier, "Inhibitors of 17b-hydroxysteroid dehydrogenases," Curr. Med. Chem. **10**, 453–477 (2003).
[8]E. Samuel, J. L. Atwood, W. E. Hunter, "Cyclization of phenylpropiolic acid on titanocene. Synthesis and molecular structure of di-η_5-cyclopentadienyl(cinnamylato-C^3,O)titanium/phenylpropiolic acid (1/1), a novel titanacycle. Synthesis of dicyclopentadienylbis(phenylpropiolato)titanium," J. Organomet. Chem. **311**, 325–331 (1986), Dc 1.34.
[9]C. L. Li, W. Q. Zhang, X. Qi, J. B. Peng, and X. F. Wu, "Palladium-catalyzed carbonylative synthesis of alkynones from aryl iodides and phenylpropiolic acid employing formic acid as the CO source," J. Organomet. Chem. **838**, 9–11 (2017).
[10]A. Pyo, Y. H. Kim, K. Park, G. C. Kim, H. C. Choi, and S. Lee, "Mechanistic study of palladium-catalyzed decarboxylative coupling of phenylpropiolic acid and aryl iodide," Appl. Organomet. Chem. **26**, 650–654 (2012).
[11]Y. Xie, B. F. He, N. Y. Huang, and W. Q. Deng, "The direct carboxylation of terminal alkynes with carbon dioxide using copper-conjugated microporous polymer as catalyst," Adv. Mater. Res. **634–638**, 612–615 (2013).
[12]L. Shi, W. Jia, X. Li, and N. Jiao, "Cu-catalyzed decarboxylative coupling of propiolic acids with boronic acids," Tetrahedron Lett. **54**, 1951–1955 (2013).
[13]D. L. Priebbenow, P. Becker, and C. Bolm, "Copper-catalyzed oxidative decarboxylative couplings of sulfoximines and aryl propiolic acids," Org. Lett. **15**, 6155–6157 (2013).
[14]G. Rong, J. Mao, H. Yan, Y. Zheng, and G. Zhang, "Phosphoric acid-mediated synthesis of vinyl sulfones through decarboxylative coupling reactions of sodium sulfinates with phenylpropiolic acids," J. Org. Chem. **80**, 7652–7657 (2015).

[15]K. Park, T. Palani, A. Pyo, and S. Lee, "Synthesis of aryl alkynyl carboxylic acids and aryl alkynes from propiolic acid and aryl halides by site selective coupling and decarboxylation," Tetrahedron Lett. **53**, 733–737 (2012).
[16]K. M. Shamsuddin, M. Jamshed Ahmed Siddiqui, and A. Siddiqui, J. Chem. Res. **6**, 392–393 (1998).
[17]D. I. Nilov and A. V. Vasilyev, "One-pot tandem hydrophenylation and ionic hydrogenation of 3-phenylpropynoic acid derivatives under superelectrophilic activation," Tetrahedron Lett. **56**, 5714–5717 (2015).
[18]T. Takano-Yamamoto and G. A. Rodan, "Direct effects of 17 beta-estradiol on trabecular bone in ovariectomized rats," Proc. Natl. Acad. Sci. U. S. A. **87**, 2172–2176 (1990).
[19]M. Zieliński, A. Zielińska, H. Papiernik-Zielińska, N. Ogrinc, and I. Kobal, "Carbon isotope fractionation in the decarboxylation of phenylpropiolic acid in hydrogen donating media," Isot. Environ. Health Stud. **37**, 239–252 (2001).
[20]M. J. S. Monte and D. M. Hillesheim, "Thermodynamic study on the sublimation of 1,2-diphenylethane and of 3-phenylpropiolic acid," J. Chem. Thermodyn. **33**, 849–857 (2001).
[21]J. S. Rollett, "The crystal structure of phenyl-propiolic acid," Acta Crystallogr. **8**, 487 (1955).
[22]D. Das and G. R. Desiraju, "Packing modes in some mono- and disubstituted phenylpropiolic acids: Repeated occurrence of the rare *syn,anti* catemer," Chem. - Asian J. **1**, 231–244 (2006).
[23]D. Das, R. K. R. Jetti, R. Boese, and G. R. Desiraju, "Stereoelectronic effects of substituent groups in the solid state. Crystal chemistry of some cubanecarboxylic and phenylpropiolic acids," Cryst. Growth Des. **3**, 675–681 (2003).
[24]Z. Zhou, A. M. Pejlovas, W. Lin, and S. G. Kukolich, "The microwave spectrum of phenylpropiolic acid," J. Mol. Spectrosc. **351**, 1–3 (2018).
[25]M. J. Frisch, G. W. Trucks, H. B. Schlegel, G. E. Scuseria, M. A. Robb, J. R. Cheeseman, G. Scalmani, V. Barone, B. Mennucci, G. A. Petersson, H. Nakatsuji, M. Caricato, X. Li, H. P. Hratchian, A. F. Izmaylov, J. Bloino, G. Zheng, J. L. Sonnenberg, M. Hada, M. Ehara, K. Toyota, R. Fukuda, J. Hasegawa, M. Ishida, T. Nakajima, Y. Honda, O. Kitao, H. Nakai, T. Vreven, J. A. Montgomery, Jr., J. E. Peralta, F. Ogliaro, M. Bearpark, J. J. Heyd, E. Brothers, K. N. Kudin, V. N. Staroverov, R. Kobayashi, J. Normand, K. Raghavachari, A. Rendell, J. C. Burant, S. S. Iyengar, J. Tomasi, M. Cossi, N. Rega, J. M. Millam, M. Klene, J. E. Knox, J. B. Cross, V. Bakken, C. Adamo, J. Jaramillo, R. Gomperts, R. E. Stratmann, O. Yazyev, A. J. Austin, R. Cammi, C. Pomelli, J. W. Ochterski, R. L. Martin, K. Morokuma, V. G. Zakrzewski, G. A. Voth, P. Salvador, J. J. Dannenberg, S. Dapprich, A. D. Daniels, Ö. Farkas, J. B. Foresman, J. V. Ortiz, J. Cioslowski, and D. J. Fox, Gaussian 09, Revision D.01, 2009.
[26]M. J. Frisch, G. W. Trucks, H. B. Schlegel, G. E. Scuseria, M. A. Robb, J. R. Cheeseman, G. Scalmani, V. Barone, G. A. Petersson, H. Nakatsuji, X. Li, M. Caricato, D. J. F. A. V. Marenich, J. Bloino, B. G. Janesko, R. Gomperts, B. Mennucci, H. P. Hratchian, and J. V. Izmaylov, Gaussian 16, Revision B.01, 2016.
[27]S. H. Vosko, L. Wilk, and M. Nusair, "Accurate spin-dependent electron liquid correlation energies for local spin density calculations: A critical analysis," Can. J. Phys. **58**, 1200–1211 (1980).
[28]A. D. Becke, "Density-functional exchange-energy approximation with correct asymptotic behavior," Phys. Rev. A **38**, 3098–3100 (1988).
[29]C. Lee, W. Yang, and R. G. Parr, "Development of the Colle-Salvetti correlation-energy formula into a functional of the electron density," Phys. Rev. B **37**, 785–789 (1988).
[30]C. Møller and M. S. Plesset, "Note on an approximation treatment for many-electron systems," Phys. Rev. **46**, 618–622 (1934).
[31]A. D. McLean and G. S. Chandler, "Contracted Gaussian basis sets for molecular calculations. I. Second row atoms, $Z = 11–18$," J. Chem. Phys. **72**, 5639–5648 (1980).
[32]R. Krishnan, J. S. Binkley, R. Seeger, and J. A. Pople, "Self-consistent molecular orbital methods. XX. A basis set for correlated wave functions," J. Chem. Phys. **72**, 650–654 (1980).
[33]M. J. Frisch, J. A. Pople, and J. S. Binkley, "Self-consistent molecular orbital methods 25. Supplementary functions for Gaussian basis sets," J. Chem. Phys. **80**, 3265–3269 (1984).
[34]T. Clark, J. Chandrasekhar, G. W. Spitznagel, and P. V. R. Schleyer, "Efficient diffuse function-augmented basis sets for anion calculations. III. The 3-21+G basis set for first-row elements, Li–F," J. Comput. Chem. **4**, 294–301 (1983).
[35]T. H. Dunning, "Gaussian basis sets for use in correlated molecular calculations. I. The atoms boron through neon and hydrogen," J. Chem. Phys. **90**, 1007–1023 (1989).
[36]R. A. Kendall, T. H. Dunning, and R. J. Harrison, "Electron affinities of the first-row atoms revisited. Systematic basis sets and wave functions," J. Chem. Phys. **96**, 6796–6806 (1992).
[37]C. Peng and H. Bernhard Schlegel, "Combining synchronous transit and quasi-Newton methods to find transition states," Isr. J. Chem. **33**, 449–454 (1993).
[38]Chemcraft—Graphical Software for Visualization of quantum Chemistry Computations; https://www.chemcraftprog.com.
[39]G. Ogruc Ildiz and R. Fausto, "Structural aspects of the *ortho* chloro- and fluoro-substituted benzoic acids: Implications on chemical oroperties," Molecules **25**, 4908 (2020).
[40]R. Fausto, L. A. E. B. de Carvalho, J. J. C. Teixeira-Dias, and M. N. Ramos, "S-*cis* and s-*trans* conformers of formic, thioformic and dithioformic acids. An *ab initio* study," J. Chem. Soc., Faraday Trans. 2 **85**, 1945–1962 (1989).
[41]R. Fausto, "Bonding in carbonyl and thiocarbonyl compounds: An *ab initio* charge density study of $H_2C{=}X$ and HC(=X)YH (X, Y=O or S)," J. Mol. Struct.: THEOCHEM **315**, 123–136 (1994).
[42]J. J. C. Teixeira-Dias and R. Fausto, "A molecular mechanics force field for conformational analysis of simple acyl chlorides, carboxylic acids and esters," J. Mol. Struct. **144**, 199–213 (1986).
[43]R. Fausto, G. O. Ildiz, and C. M. Nunes, "IR-induced and tunneling reactions in cryogenic matrices: The (incomplete) story of a successful endeavor," Chem. Soc. Rev. **51**, 2853–2872 (2022).
[44]G. Bazsó, S. Góbi, and G. Tarczay, "Near-infrared radiation induced conformational change and hydrogen atom tunneling of 2-chloropropionic acid in low-temperature Ar matrix," J. Phys. Chem. A **116**, 4823–4832 (2012).
[45]I. D. Reva, S. G. Stepanian, L. Adamowicz, and R. Fausto, "Conformational behavior of cyanoacetic acid: A combined matrix isolation fourier transform infrared spectroscopy and theoretical study," J. Phys. Chem. A **107**, 6351–6359 (2003).
[46]R. F. G. Apóstolo, G. Bazsó, G. O. Ildiz, G. Tarczay, and R. Fausto, "Near-infrared *in situ* generation of the higher-energy *trans* conformer of tribromoacetic acid: Observation of a large-scale matrix-site changing mediated by conformational conversion," J. Chem. Phys. **148**, 044303 (2018).